Applying spatial attention-based autoencoder learning of latent representation for unsupervised characterization of tumor microenvironment

Abstract

Spatial tissue imaging technologies enable highly resolved spatial characterization of cellular phenotypes however today it depends on laborious manual annotation and molecular labels to understand tissue organization. As a result, we are not optimally leveraging higher-order patterns of cell organization potentially connected to disease pathology. Our approach combines information on cellular phenotypes with the physical proximity of cells to accurately identify organ-specific microanatomical in the tumor microenvironment.

Keywords: Autoencodeurs, spatial attention, computational pathology

1. Introduction

Spatial biology applications are advancing the study of tissue organization and cell2cell communication at an unprecedented scale. New tools are required to store, analyze and visualize the large diversity of produced data(Barmpoutis et al., 2021)(Ahmedt-Aristizabal et al., 2022). Autoencoders (AE) have been used to visualize or generate interpretable embeddings from biological single-cell data, an example is scvis(Ding et al., 2018)(Becht et al., 2019). More recently, new autoencoder models, in particular graph-based AE, use spatial information along with phenotypical information(Hu et al., 2021)(Dong and Zhang, 2022). But attention neural networks are becoming popular and new autoencoder models using attention mechanism have shown promising results with biological data(Dong and Zhang, 2022)(Fu et al., 2021). Imaging mass cytometry (IMC) it is a novel imaging technology, with more than 40 markers per pixel, that due the high content natures poses computational complexity challenges. Furthermore, due to the measurement protocol, the data can be noisy prone to artefacts and create biaises difficult to handle by the clustering approaches. To address all these challenges we are proposing a new approach to leverage spatial attention AE for IMC tissue structure phenotyping.

2. Materials and methods

Data: Patients included in the study are advanced stage and metastatic treated with different immune-oncology therapies(Camps et al., 2023). IMC assays were applied to selected ROIs with 40-marker panel (DAPI + 39 molecular probes) to characterize the TME. ROIs (3-4 per patient) were selected by an expert histologist to represent at high resolution (1 micro-meter) major tumor anatomical regions (Figure.1A). **Data split:** To fully leverage all available data (Table.1) we used dataset I (2 patients, 8 ROIs) for training and dataset II (39 patients, 128 ROIs) and III (139 patients, 556 ROIs) for independent testing.

Design of autoencoder experimentations: (Classic AE) The model considered as a baseline it is a regular fully connected three-layer autoencoder with a wasserstein regularization (loss term using Wasserstein distance on the embeddings)(Kolouri et al., 2018). **(Classic spatially aware AE)** For each cell, a value representing the distance to specified cell populations (annotated histological ROIs) is constructed. Outlier detections algorithms (i.e. Isolation Forest algorithm) is used to encode with min-max scaling, 1 (cell is close to a histological cluster) and 0 (it is not part a histological ROI) (Figure.1B). **(Classic spatially aware AE with attention mechanism)**. Here we introduced the attention mechanisms by assigning to a sample a linear combination of specified inputs. We emphasize attention to histological ROIs (i.e. cell populations of interest like tumor and stroma) and relative distances (Figure.1C-D). **Type of connections:** For fully connected AE all layers are full connected and input features equally weighted. For sparse connections, we introduce sparsity by enriching the model with more biological sense, thus "regrouping" features that have biological relationships(Alessandri et al., 2020). These relationships are based on expert cell annotations. In practice, this is done by enforcing sparse connections in the first layer of the encoder. Hidden nodes of the first layer only receive inputs from the nodes associated to this node (Figure.1B). **Hyperparameter tunning and clustering:** Model hyperparameters (i.e. number of layers, dimension of the hidden layers, dimension of the latent space, batch size, Wasserstein regularization weights, learning rate, activations functions) were optimised using a grid-search paradigm (only for the spatial attention AE). A trained model for each combination (model, connections type) was used to compute the automated mutual information (AMI) out of different clustering strategies: Kmeans, Phenograph(Levine et al., 2015) and Spatialsort(Lee et al., 2022).

Loss metrics	Model	Connections	Train	Test 1	Test 2
Reconstrution error (MSE)	Classic	Fully	1.31 ± 0.04	2.13 ± 0.06	2.01 ± 0.05
		Sparse	1.67 ± 0.09	2.48 ± 0.11	2.37 ± 0.10
	Classic Spatial	Fully	1.48 ± 0.04	2.58 ± 0.07	2.38 ± 0.07
		Sparse	1.84 ± 0.08	2.99 ± 0.14	2.76 ± 0.12
	Spatial Attention	Fully	1.44 ± 0.05	2.28 ± 0.06	2.17 ± 0.06
		Sparse	1.84 ± 0.10	2.65 ± 0.11	2.55 ± 0.11

Table 1: Reconstruction error and comparison between different autoencoders.

3. Results

The results (Table 1) were smoothed with 50 iterations per model and the sliced-Wasserstein distance was evaluated 50 times for each embedding. The values are presented as mean ± std. The autoencoder succeeds in capturing important features of the data. The original data is indeed well reconstructed from embeddings of dimension 16 (versus an original dimension of 43). The regularization using Wasserstein distance enables the latent space to have the shape of a Gaussian distribution, which is beneficial for the clustering techniques (Figure.1E). Sparse connections and spatial information impact is however harder to notice. Hard to analyse the results concerning clustering as there is no ground truth novels phenotypes.
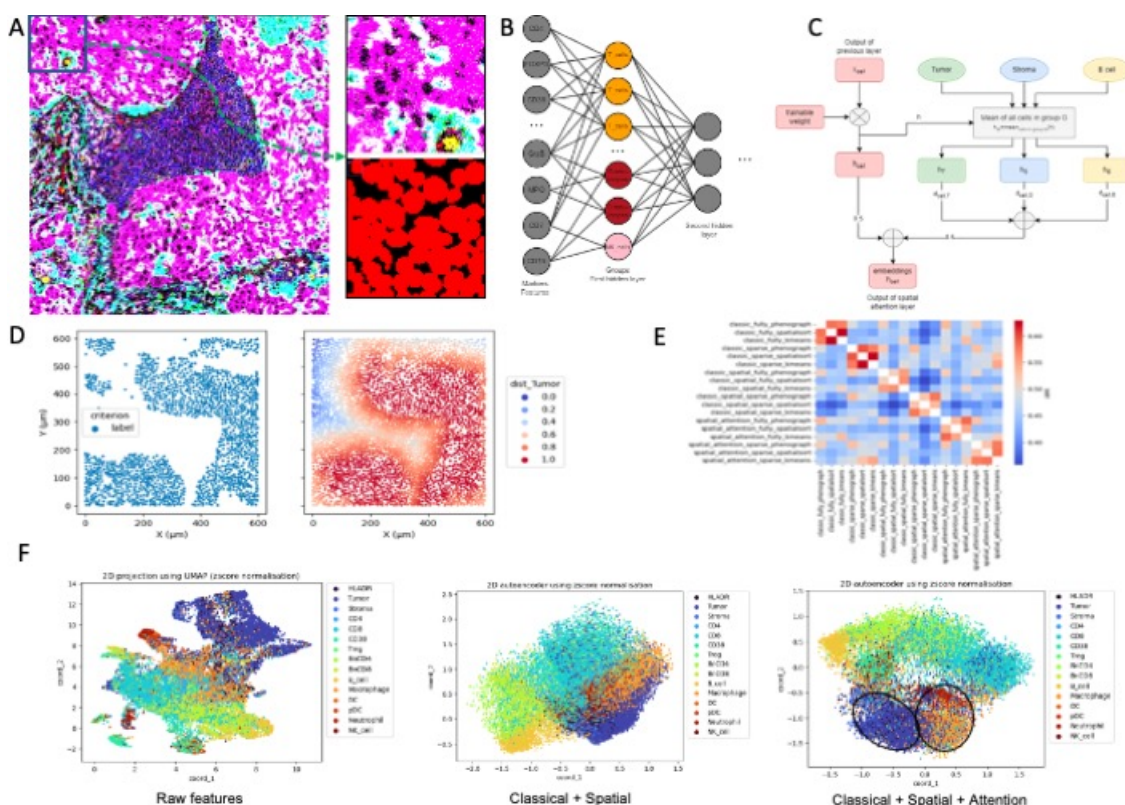
Figure 1: Latent representation. A) Illustration of selected channels from raw IMC as well as high power field and mask of selected region. B) Design of sparse connections guided by biological rationale. C) Spatial attention mechanism using major histological regions as anchors. D) Illustration of a ground truth histological ROIs. E) Clustering AMI criteria based on different AE. F) 2D projections of cells (sampled from the training dataset I) using normalised raw features (left) and AE embeddings with spatial information integrated (middle) as well as attention mechanism (right).

4. Conclusions

Our experiments shows that AE succeeds in capturing important features of the data however the impact of spatial information it is harder to notice using AMI or the Wasserstein distance and by selecting a specific region as well as other evaluation metric. The influence of the model and the type of connections (sparse or full) can clearly observed when looking at the overlay of cell phenotypes labels on AE embeddings (Figure.1F). The different cell populations are more well defined with AE (middle and right graphics). The overlapping cell phenotypes (indicated with black oval shapes in Figure.1F) within tumour we can identify a cluster of cells with both DC and tumour cell inside recently shown to highlights a patient not-likely to respond to immune therapies(Cohen et al., 2022)(Oh et al., 2020).

Acknowledgments

References

David Ahmedt-Aristizabal, Mohammad Ali Armin, Simon Denman, Clinton Fookes, and Lars Petersson. A survey on graph-based deep learning for computational histopathology. *Computerized Medical Imaging and Graphics*, 95:102027, 2022. ISSN 0895-6111. doi: 10.1016/j.compmedimag.2021.102027.

Luca Alessandri, Francesca Cordero, Marco Beccuti, Nicola Licheri, Maddalena Arigoni, Martina Olivero, Maria Flavia Di Renzo, Anna Sapino, and Raffaele Calogero. Sparsely-connected autoencoder (SCA) for single cell RNAseq data mining. *NPJ systems biology and applications*, 7(1):1, 2020. doi: 10.1038/s41540-020-00162-6.

Panagiotis Barmpoutis, Matthew Di Capite, Hamzeh Kayhanian, William Waddingham, Daniel C. Alexander, Marnix Jansen, and Francois Ng Kee Kwong. Tertiary lymphoid structures (TLS) identification and density assessment on H&E-stained digital slides of lung cancer. *PLoS ONE*, 16(9):e0256907, 2021. doi: 10.1371/journal.pone.0256907.

Etienne Becht, Leland McInnes, John Healy, Charles-Antoine Dutertre, Immanuel W H Kwok, Lai Guan Ng, Florent Ginhoux, and Evan W Newell. Dimensionality reduction for visualizing single-cell data using UMAP. *Nature Biotechnology*, 37(1):38–44, 2019. ISSN 1087-0156. doi: 10.1038/nbt.4314.

Jordi Camps, Floriane Noël, Robin Liechti, Lucile Massenet-Regad, Sidwell Rigade, Lou Götz, Caroline Hoffmann, Elise Amblard, Melissa Saichi, Mahmoud M. Ibrahim, Jack Pollard, Jasna Medvedovic, Helge G. Roider, and Vassili Soumelis. Meta-Analysis of Human Cancer Single-Cell RNA-Seq Datasets Using the IMMUcan Database. *Cancer Research*, 83(3):OF1–OF11, 2023. ISSN 0008-5472. doi: 10.1158/0008-5472.can-22-0074.

Merav Cohen, Amir Giladi, Oren Barboy, Pauline Hamon, Baoguo Li, Mor Zada, Anna Gurevich-Shapiro, Cristian Gabriel Beccaria, Eyal David, Barbara B. Maier, Mark Buckup, Iris Kamer, Aleksandra Deczkowska, Jessica Le Berichel, Jair Bar, Matteo Iannacone, Amos Tanay, Miriam Merad, and Ido Amit. The interaction of CD4+ helper T cells with dendritic cells shapes the tumor microenvironment and immune checkpoint blockade response. *Nature Cancer*, 3(3):303–317, 2022. doi: 10.1038/s43018-022-00338-5.

Jiarui Ding, Anne Condon, and Sohrab P. Shah. Interpretable dimensionality reduction of single cell transcriptome data with deep generative models. *Nature Communications*, 9 (1):2002, 2018. doi: 10.1038/s41467-018-04368-5.

Kangning Dong and Shihua Zhang. Deciphering spatial domains from spatially resolved transcriptomics with an adaptive graph attention auto-encoder. *Nature Communications*, 13(1):1739, 2022. doi: 10.1038/s41467-022-29439-6.

Huazhu Fu, Hang Xu, Kelvin Chong, Mengwei Li, Kok Siong Ang, Hong Kai Lee, Jingjing Ling, Ao Chen, Ling Shao, Longqi Liu, and Jinmiao Chen. Unsupervised Spatially Embedded Deep Representation of Spatial Transcriptomics. *bioRxiv*, page 2021.06.15.448542, 2021. doi: 10.1101/2021.06.15.448542.

Jian Hu, Xiangjie Li, Kyle Coleman, Amelia Schroeder, Nan Ma, David J. Irwin, Edward B. Lee, Russell T. Shinohara, and Mingyao Li. SpaGCN: Integrating gene expression, spatial location and histology to identify spatial domains and spatially variable genes by graph convolutional network. *Nature Methods*, 18(11):1342–1351, 2021. ISSN 1548-7091. doi: 10.1038/s41592-021-01255-8.

Soheil Kolouri, Phillip E Pope, Charles E Martin, and Gustavo K Rohde. Sliced-Wasserstein Autoencoder: An Embarrassingly Simple Generative Model. *arXiv*, 2018. doi: 10.48550/arxiv.1804.01947.

Eric Lee, Kevin Chern, Michael Nissen, Xuehai Wang, IMAXT Consortium, Chris Huang, Anita K Gandhi, Alexandre Bouchard-Côté, Andrew P Weng, and Andrew Roth. SpatialSort: A Bayesian Model for Clustering and Cell Population Annotation of Spatial Proteomics Data. *bioRxiv*, page 2022.07.27.499974, 2022. doi: 10.1101/2022.07.27.499974.

Jacob H. Levine, Erin F. Simonds, Sean C. Bendall, Kara L. Davis, El-ad D. Amir, Michelle D. Tadmor, Oren Litvin, Harris G. Fienberg, Astraea Jager, Eli R. Zunder, Rachel Finck, Amanda L. Gedman, Ina Radtke, James R. Downing, Dana Pe'er, and Garry P. Nolan. Data-Driven Phenotypic Dissection of AML Reveals Progenitor-like Cells that Correlate with Prognosis. *Cell*, 162(1):184–197, 2015. ISSN 0092-8674. doi: 10.1016/j.cell.2015.05.047.

Soyoung A. Oh, Dai-Chen Wu, Jeanne Cheung, Armando Navarro, Huizhong Xiong, Rafael Cubas, Klara Totpal, Henry Chiu, Yan Wu, Laetitia Comps-Agrar, Andrew M. Leader, Miriam Merad, Merone Roose-Germa, Soren Warming, Minhong Yan, Jeong M. Kim, Sascha Rutz, and Ira Mellman. PD-L1 expression by dendritic cells is a key regulator of T-cell immunity in cancer. *Nature Cancer*, 1(7):681–691, 2020. doi: 10.1038/s43018-020-0075-x.